



Deposited via The University of Leeds.

White Rose Research Online URL for this paper:

<https://eprints.whiterose.ac.uk/id/eprint/176494/>

Version: Accepted Version

Article:

Adnan, MSG, Dewan, A, Zannat, KE et al. (2019) The use of watershed geomorphic data in flash flood susceptibility zoning: a case study of the Karnaphuli and Sangu river basins of Bangladesh. *Natural Hazards*, 99 (1). pp. 425-448. ISSN: 0921-030X

<https://doi.org/10.1007/s11069-019-03749-3>

© Springer Nature B.V. 2019. This is an author produced version of an article published in *Natural Hazards*. Uploaded in accordance with the publisher's self-archiving policy.

Reuse

Items deposited in White Rose Research Online are protected by copyright, with all rights reserved unless indicated otherwise. They may be downloaded and/or printed for private study, or other acts as permitted by national copyright laws. The publisher or other rights holders may allow further reproduction and re-use of the full text version. This is indicated by the licence information on the White Rose Research Online record for the item.

Takedown

If you consider content in White Rose Research Online to be in breach of UK law, please notify us by emailing eprints@whiterose.ac.uk including the URL of the record and the reason for the withdrawal request.

1 **The use of watershed geomorphic data in flash flood susceptibility zoning: a case study**
2 **of the Karnaphuli and Sangu river basins of Bangladesh**

3 **Abstract**

4 The occurrence of heavy rainfall in the south-eastern hilly region of Bangladesh makes this area highly
5 susceptible to recurrent flash flooding. As the region is the commercial capital of Bangladesh, these
6 flash floods pose a significant threat to the national economy. Predicting this type of flooding is a
7 complex task which requires a detailed understanding of the river basin characteristics. This study
8 evaluated the susceptibility of the region to flash floods emanating from within the Karnaphuli and
9 Sangu river basins. Twenty-two morphometric parameters were used. The occurrence and impact of
10 flash floods within these basins is mainly associated with the volume of runoff, runoff velocity, and the
11 surface infiltration capacity of the various watersheds. Analysis showed that major parts of the basin
12 were susceptible to flash flooding events of a ‘moderate’ to ‘very high’ level of severity. The degree of
13 susceptibility of ten of the watersheds was rated as ‘high’, and one was ‘very high’. The flash flood
14 susceptibility map drawn from the analysis was used at the sub-district level to identify populated areas
15 at risk. More than 80% of the total area of the 16 sub-districts were determined to have a ‘high’ to ‘very
16 high’ level flood susceptibility. The analysis noted that around 3.4 million people reside in flash flood
17 prone areas, therefore indicating the potential for loss of life and property. The study identified
18 significant flash flood potential zones within a region of national importance, and exposure of the
19 population to these events. Detailed analysis and display of flash flood susceptibility data at the sub-
20 district level can enable the relevant organizations to improve watershed management practices and, as
21 a consequence, alleviate future flood risk.

22 Keywords: Flash flood; watershed hydrology; morphometric analysis; geomorphology; GIS;
23 Bangladesh

24 **1. Introduction**

25 The flash flooding phenomenon, a commonly occurring natural hazard in many regions of the world,
26 poses a major threat to population, environment and infrastructure in the areas in which they occur
27 (Bajabaa et al. 2014; Elnazer et al. 2017). It is a largely localized event caused by exceptionally heavy
28 rainfall (Brammer 1990; Kamal et al. 2018), and can be accompanied by other hazards such as
29 landslides and mud flows (Collier 2007). Flash floods occur randomly in time and space and therefore
30 forecasting these events tends to be very difficult (Kron 2005). The high velocity of flood water also
31 substantially increases the potential for soil erosion, and flash floods can become a severe threat to lives
32 and property within a very short period of time (Plate 2002). Land use change, such as from
33 predominantly vegetation cover to substantially built-up, exacerbates the intensity of this type of flood
34 by increasing the generation of runoff in the catchment area and the loss of flood attenuation capacity
35 (Bronstert et al. 2002). The frequency and intensity of extreme precipitation events due to climate

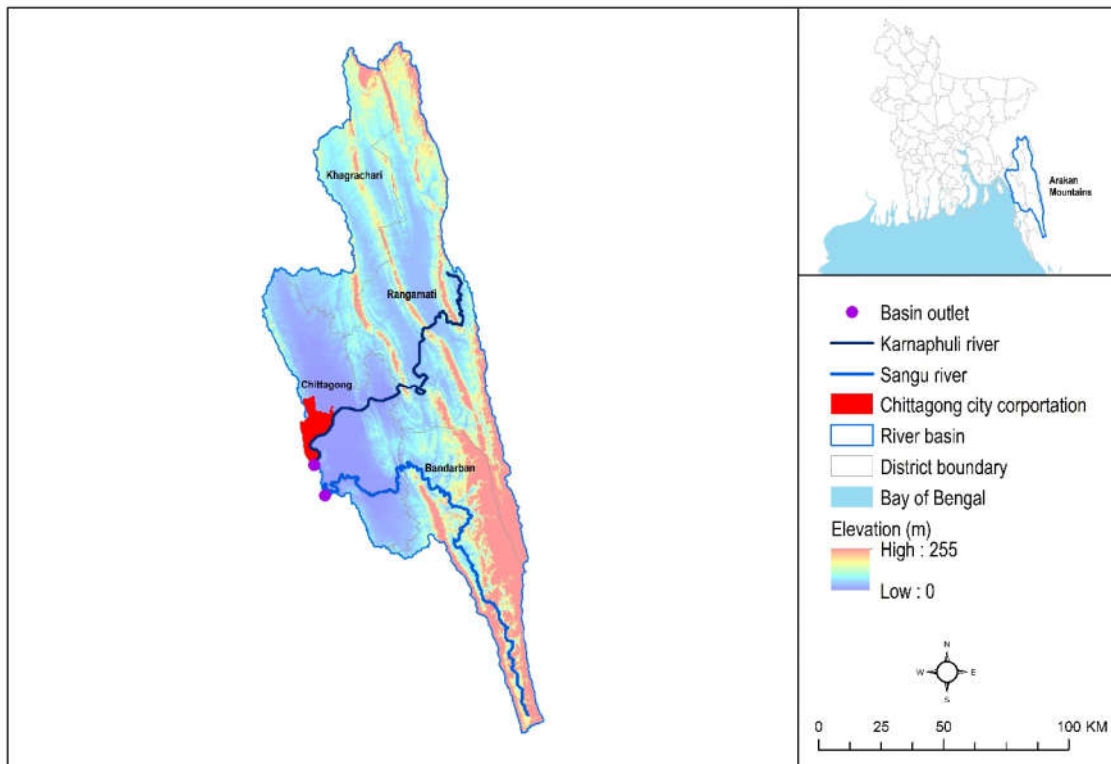
36 change are expected to increase, potentially increasing the likelihood of flash flood events in the future
37 (Adnan and Kreibich 2016; Field et al. 2012; Rahman et al. 2019).

38 The unique geographic and physiographic settings of Bangladesh make it prone to multiple flood types.
39 This includes: i) river; ii) pluvial; iii) flash; iv) tidal; and v) storm-surge induced floods (Rahman and
40 Salehin 2013). On average, 20-25% of the area is susceptible to flooding in a normal year, while extreme
41 flood events such as those that occurred in 1987, 1988, and 1998 inundated more than 60% of the total
42 land area (Dewan 2013; Dewan 2015). The socio-economic impacts of these recurrent floods are
43 significant. For the period 2009 to 2014, various flood events of different magnitudes have affected, on
44 average, 57.01% of the households in Bangladesh. The economic cost of those floods was estimated at
45 71.55 billion Bangladeshi Taka (0.85 billion USD) (BBS 2015). While several studies have been
46 conducted on river and coastal floods in Bangladesh (Adnan et al. 2019; Dewan 2013), researchers so
47 far have paid little attention to flash flooding events and impacts. Kamal et al. (2018) assessed the flash
48 flood vulnerability of the ‘Haor’ community located in the north eastern region of Bangladesh. Based
49 on available empirical data, they demonstrated that the remote location of households, lack of access to
50 accurate weather forecasting and poor housing conditions led to significant physical damage during the
51 flash floods. In the absence of empirical data, however, identification of the zones which are susceptible
52 to flash flooding requires a detailed knowledge of the physical drivers triggering such floods
53 (Choudhury et al. 2004).

54 The south eastern hilly region of Bangladesh is bordered by the Arakan mountains to the east and the
55 Bay of Bengal to the west (Choudhury et al. 2004). The commercial capital of the country, Chittagong
56 City, is located in this area and is prone to flash flooding events (Rahman and Salehin 2013). The area
57 is known as a high-risk zone as it can experience heavy rainfall which can trigger both flash floods and
58 landslides (Ahmed and Dewan 2017; Rahman et al. 2017). It should be noted that there can be a high
59 spatial-temporal variation in these occurrences. Location, topography, and localized climate can all
60 increase flooding episodes, and the additional flow through transboundary rivers has the potential to
61 increase the flood intensity (Sarker and Rashid 2013). Predicting the occurrence of such a flood type is
62 complex due to the fact that the water and associated materials can travel downstream very quickly to
63 other locations where the initial rainfall event has not been observed and the flash flood event is
64 therefore not expected (Kron 2005). An increased knowledge of causative factors could help assess the
65 flood susceptibility of an area. For instance, steep terrain tends to generate high velocity runoff, a major
66 contributor to a flash flood. Besides, geomorphic, drainage, and climatic conditions could also
67 contribute to possible causes (Elnazer et al. 2017; Youssef et al. 2011). To manage flash floods
68 effectively, morphometric factors can be used to delineate the flood-susceptible zones (Bajabaa et al.
69 2014; Rahman and Di 2017; Youssef et al. 2011). An examination of these factors is a major focus of
70 this study.

71 Morphometric analysis of watersheds is a widely-recognized approach characterizing the hydrological
 72 response of a watershed (Bajabaa et al. 2014; Farhan et al. 2017; Rai et al. 2017; Youssef et al. 2011).
 73 Several methods are commonly used to quantify watershed geomorphology; these are primarily grouped
 74 under linear measurement and dimensionless numbers (Strahler 1957). Since morphometric parameters
 75 indicate the river basin's physical behaviour when undergoing extreme precipitation events (Diakakis
 76 2011), several studies have combined the use of the various parameters when assessing the potential for
 77 flash floods and associated hazards (Bajabaa et al. 2014; Bhatt and Ahmed 2014; Elnazer et al. 2017;
 78 Youssef et al. 2011). In recent years, the use of a Geographic Information System (GIS) in combination
 79 with the availability of accurate spatial data, including remote-sensing data, has become an important
 80 decision-making tool in flood risk management (Abdullah et al. 2019; Elnazer et al. 2017; Lin et al.
 81 2019). Within Bangladesh, a number of studies have been undertaken to conceptualize flash flood
 82 vulnerability in the larger catchments (Rahman and Salehin 2013; Sarker and Rashid 2013), however
 83 researchers are yet to utilise watershed morphometric analysis to estimate flood susceptibility in the
 84 smaller watersheds. This study aims to: 1) analyse the relationship of various morphometric parameters
 85 with flash flood susceptibility at the watershed level; and 2) develop a detailed, flood susceptibility map
 86 for the area.

87



88

89

Figure 1 The Karnaphuli and Sangu river basins

90 **2. Study area**

91 The Karnaphuli and Sangu river basins, located in the south eastern hilly region of Bangladesh
92 (hereinafter, region), were selected for the study (Figure 1). These basins have total areas of 8,845.18
93 km² and 3,842.82 km², respectively. The region is made up of 40 sub-districts within the larger
94 Bandarban, Chittagong, Khagrachari, and Rangamati districts. The basins are mostly characterized by
95 brown hilly soils, with 63% of the total area being composed of this type of soil. Another 13% of the
96 area contains Non-calcareous Grey Floodplain Soils (non-saline) with 20% of the total land reserved as
97 forest (BARC 2014).

98 The region is subjected to periods of heavy rainfall annually (particularly during the monsoon season)
99 making it very prone to flash floods. The mean annual precipitation in Chittagong district, for example,
100 is about 2,917 mm (Ahmed and Dewan 2017), signifying a high potential for flash floods events. Several
101 of these rainfall-induced events have previously been reported to have affected either the whole or part
102 of the two basins (Brakenridge 2018). From 1985 until 2015, heavy rainstorms badly affected the region
103 a total of 12 times (Table 1). These events had a massive, negative impact on both population and
104 property. For example, the torrential rain event of 23rd June 2015 triggered a flash flood that affected
105 approximately 1.8 million people in 29 sub-districts of the Chittagong, Bandarban, and Cox’s bazar
106 districts. A post-disaster relief and rehabilitation effort was the main government response (ACAPS
107 2015). Biswas et al. (2012) developed an integrated watershed management (IWM) scheme for
108 Chittagong hill tracts, and included flood control at the watershed scale as one of the major mitigation
109 strategies. Since the impact of flash floods tends to be heterogeneous across different administrative
110 units, the development of a susceptibility map at the watershed scale has been suggested as a measure
111 to provide assistance to local managers in the operational planning phase. It could not only show the
112 spatial variability of hazards on a smaller administrative scale, but could also help resource managers
113 to control the associated risks more effectively.

114 Table 1 Major flash flood events reported in the south-eastern hilly region

Year	Location (districts)	Cause	Number of people affected	Source
1985	Chittagong	Heavy rain	77000	(Brakenridge 2018)
1988	Chittagong	Heavy rain	15000	(Brakenridge 2018)
1989	Chittagong, Bandarban,	Monsoonal rain	20000	(Brakenridge 2018)
1990	Chittagong, Cox’s Bazar	Heavy rain	310000	(Brakenridge 2018)
1991	Chittagong, Cox’s Bazar	Heavy rain	50000	(Brakenridge 2018)
1992	Chittagong	Monsoonal rain	50000	(Brakenridge 2018)

1994	Chittagong	Heavy rain	12000	(Brakenridge 2018)
1997	Chittagong, Bandarban, Rangamati, Cox's bazar	Heavy rain	239000	(Brakenridge 2018)
2000	Chittagong, Bandarban, Khagrachari, Rangamati, Cox's bazar	Monsoonal rain, torrential rain	30000	(Brakenridge 2018; Sarker and Rashid 2013)
2003	Chittagong, Khagrachari, Cox's bazar	Monsoonal rain	20000	(Brakenridge 2018; Sarker and Rashid 2013)
2012	Chittagong, Bandarban, Cox's bazar	Monsoonal rain	102000	(Brakenridge 2018; Sarker and Rashid 2013)
2015	Chittagong, Bandarban, Cox's Bazar	Torrential rain	1800000	(ACAPS 2015; Brakenridge 2018)

115

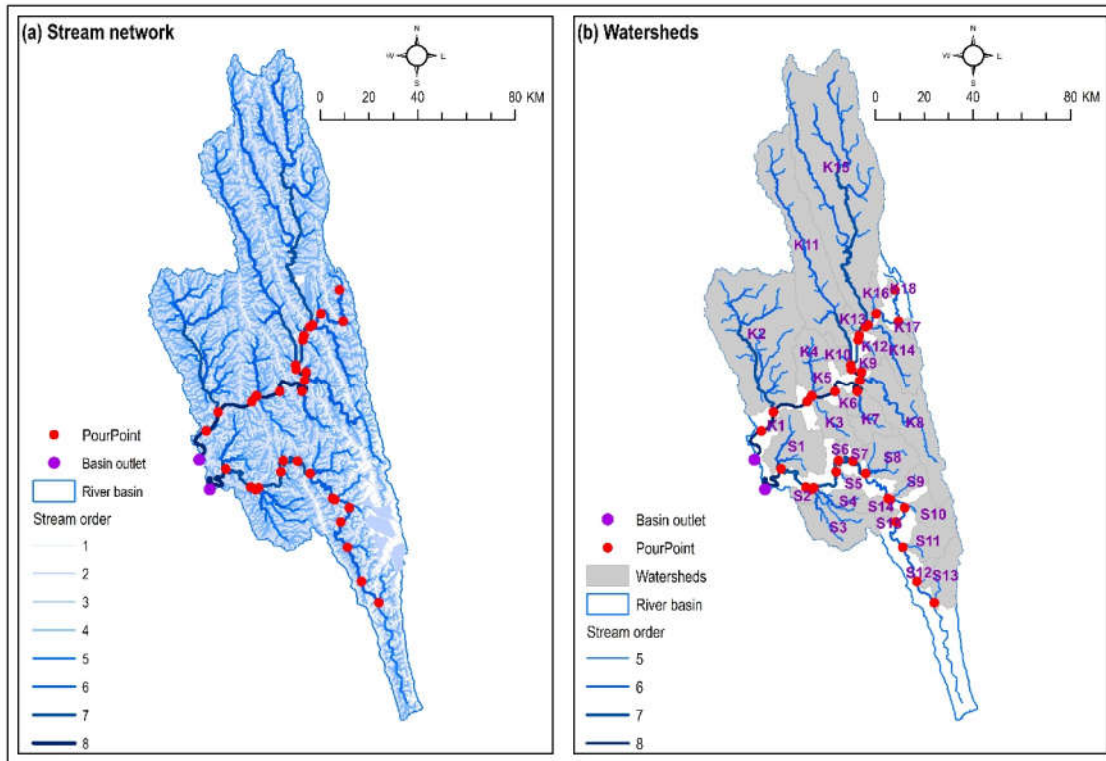
116 **3. Materials and methods**

117 **3.1. Extraction of river basins**

118 A SRTM (Shuttle Radar Topographic Mission) digital elevation model (DEM) with a spatial resolution
 119 of 30 m was obtained from EarthExplorer (<https://earthexplorer.usgs.gov/>). During subsequent
 120 processing to delineate watersheds, the sinks (errors) were removed and the drainage network was
 121 derived (Planchon and Darboux 2002). A flow direction raster was obtained by applying the single-
 122 direction flow algorithm (D8) (Seibert and McGlynn 2007). Two outlets of the Karnaphuli and Sangu
 123 basins were selected and boundaries generated (Figure 1).

124 **3.2. Extraction of drainage streams and delineating watersheds**

125 Watersheds were delineated in the two river basins using the derived drainage networks. The elevation
 126 of the extracted river basin was masked and the flow direction raster retrieved. A flow accumulation
 127 grid was generated, with each cell indicating the accumulated sums of water flowing down-slope
 128 (Kabenge et al. 2017). To create the drainage streams, a user-defined minimum threshold flow
 129 accumulation value of 100 was used (Wieczorek 2012). Subsequently a stream order was assigned by
 130 applying a stream ordering method (Strahler 1952). Strahler's ordering system assigns 1st order to
 131 streams without tributaries, 2nd order to streams with at least two 1st order tributaries, 3rd order with at
 132 least two 2nd order tributaries and so on (Hughes et al. 2011). Finally, an eight-order stream system was
 133 used to characterize the Karnaphuli and Sangu river basins (Figure 2a).



135

136

Figure 2 Stream network and watersheds of the Karnaphuli and Sangu river basin

137 The creation of a stream network was followed by the use of user-supplied pour points to delineate
 138 those points containing the highest water-shed flow accumulation (Rai et al. 2017). Pour points were
 139 identified on the basis that the calculated watersheds cover the whole river basins. According to Horton
 140 (1945), a well-drained basin contains 5th order stream channels; following this principle, pour points
 141 were selected in order to create watersheds of at least 5th order stream channels. Thirty-three watersheds
 142 were produced; 17 small (<100 km² area) and 16 large drainage basins (≥100 km² area) (Figure 2b).

143

3.3. Identifying morphometric parameters

144 Basin morphometric parameters provide essential information which allow the characterisation of
 145 hydro-meteorological hazards like floods (Shen et al. 2017). There is no defined, standard set of
 146 parameters that can be used for mapping flash flood susceptibility. In the literature, it is evident that
 147 different combinations of morphometric parameters have been used to determine flood hazard zones.
 148 For instance, Bajabaa et al. (2014) evaluated 26 morphometric parameters related to linear, areal, and
 149 relief characteristics. Similarly, Abdel-Fattah et al. (2017) analysed 38 parameters grouped under four
 150 classes as scale, topographic, shape and drainage network parameters. In this study, 29 morphometric
 151 parameters were selected under the four broad classes proposed by Abdel-Fattah et al. (2017) that
 152 provided a comprehensive picture of each drainage basin. The values of selected parameters were

153 obtained using the corresponding equations, calculated using a GIS. Table 2 shows selected
154 morphometric parameters along with the associated equations.

155 Four ‘scale’ parameters were selected: i) basin area, ii) perimeter, iii) basin length, and iv) time of
156 concentration. Basin area is a common parameter used to estimate stream discharge. This normally
157 demonstrates a strong positive correlation with peak discharge as a bigger basin will receive a higher
158 amount of precipitation, and therefore will generate a larger pulse of runoff (Abdel-Fattah et al. 2017).
159 Time of concentration indicates the time that water is needed to reach the outlet (Bhatt and Ahmed
160 2014). An inverse correlation exists between the time of concentration and runoff generation. A longer
161 time of concentration of a basin means a higher probability of ground water recharge, hence less runoff
162 (Bajabaa et al. 2014).

163 Various topographic parameters, including slope, elevation, relief and ruggedness number can influence
164 flash flood occurrence. For instance, a steep slope increases the speed of runoff, therefore increasing
165 the probability of inundation of areas with relatively gentle slope and elevation (Kabenge et al. 2017).
166 On the other hand, a low surface slope reduces runoff velocity, providing a greater degree of surface
167 infiltration and water recharge, and lowering peak flow (Bajabaa et al. 2014). A ruggedness number is
168 the product of drainage density and relief divided by 1000. A ruggedness <1 means smooth topography,
169 a value of 1-2 indicates sharper topography, and extreme values (>2) indicate ‘badland’ (areas where
170 the bedrock is poorly cemented) topography. Watersheds with a high ruggedness number therefore
171 receive a higher discharge, leading to a greater probability of flash flooding occurring (Farhan et al.
172 2017).

173 The values of different shape parameters can also explain the volume and intensity of runoff in
174 watersheds. One such parameter is the form factor which characterises the runoff intensity in a basin.
175 The higher the form factor value, the less the elongation of a basin, meaning that flow peaks over a
176 shorter time period. The form factor value of a perfectly circular basin should be less than 0.79 (Farhan
177 et al. 2017). The elongation ratio is “the ratio between the diameter of a circle with the same area as the
178 basin and the maximum length of the basin as measured for the relief ratio” (Schumm 1956). It
179 maintains an inverse relationship with flash flood as, for a given rainfall event, the basin with the smaller
180 elongation ratio will generate a higher peak discharge. The elongation ratio can vary from 0.6-1.0, with
181 a value close to 1.0 indicating low basin relief (Stralher 1964). Another shape parameter is the
182 circularity ratio, which denotes the ratio of a circumference of a circle having the same area as the
183 catchment to its perimeter (Schumm 1956). This ratio carries a positive correlation with runoff
184 generation as watersheds with a higher circularity ratio are characterized by high relief, are less
185 elongated, and less permeable, and hence have a higher probability of generating a greater quantity of
186 runoff (Farhan et al. 2017).

187 The runoff generation potential of a basin also varies with the different properties of stream systems.
 188 For instance, stream numbers are positively correlated with volume of runoff (Youssef et al. 2011). The
 189 total stream length of different watersheds is a major hydrological property that positively influences
 190 generation of runoff (Farhan et al. 2017). Longer stream length is responsible for a higher volume of
 191 runoff, leading to a flash flood occurrence (Bajabaa et al. 2014; Youssef et al. 2011). Stream frequency
 192 is defined as the number of streams per unit of basin area and drainage density is the ratio of total
 193 streams length to a basin area (Horton 1945). These two parameters are positively correlated with
 194 generation of runoff (Farhan et al. 2017). Generally, watersheds with low drainage density create
 195 suitable conditions for infiltration. Conversely, high stream frequency refers to areas of impermeable
 196 sub-surface material and reduced infiltration capacity (Youssef et al. 2011). The usefulness of drainage
 197 density and stream frequency, however, is limited when used to compare the drainage morphometric
 198 characteristics between large and small basins. For instance, the number of streams per unit of basin
 199 area could be the same for both a large and a small basin (Horton 1945). This limitation can be overcome
 200 by estimating the texture ratio, a metric denoting the ratio of stream number to basin perimeter (Smith
 201 1950). Lower values of texture ratio are associated with lower degrees of slope which create a more
 202 favourable environment for infiltration, and thus, low runoff (Bajabaa et al. 2014). The weighted mean
 203 bifurcation ratio is the final parameter that characterises stream systems in various watersheds. The
 204 bifurcation ratio is defined as “the average number of branching or bifurcations of streams of a given
 205 order to that of streams of the next lower order” (Horton 1945), which has an inverse relationship with
 206 runoff generation (Bajabaa et al. 2014).

207 Table 2 Morphometric parameters and corresponding equations

Parameters	Symbol	Equation / explanation	Equation Source
Scale parameters			
Basin area (km ²)	A	Area of each watershed	
Perimeter (km)	P	Perimeter of each watershed	
Basin length (km)	L _b	Maximum length of each watershed	
Time of concentration	T _c	$T_c = 0.542(L_{ms}/S_{ms})^2$	(Abdel-Fattah et al. 2017)
Topographic parameter			
Mean elevation (m)	H _m	Mean elevation of each watershed	
Maximum elevation (m)	H _{max}	Maximum elevation of each watershed	
Basin mouth elevation (m)	H _{min}	Elevation at pour points	

Total Basin Relief (m)	R	$R = (H_{max} - H_{min})$	(Schumm 1956)
Relief ratio	R_{hl}	$R_{hl} = R/L_b$	(Schumm 1956)
Ruggedness number	R_n	$R_n = D_d \times (R/1000)$	(Melton 1957)
Mean basin slope	S_b	Average slope of each watershed	
Mainstream slope	S_{ms}	Average mainstream slope of each watershed	
Slope ratio	S_r	$S_r = S_{ms}/S_b$	(Horton 1945)
Longest stream slope	S_{ls}	Average slope of longest stream in each watershed	
Shape parameters			
Form factor	F	$F = A/L_b^2$	(Horton 1932)
Compactness ratio	C	$C = P/2\sqrt{\pi A}$	(Horton 1932)
Circularity ratio	R_c	$R_c = 4\pi A/P^2$	(Schumm 1956)
Elongation ratio	R_e	$2\sqrt{A/\pi}/L_b$	(Schumm 1956)
Drainage network parameters			
Stream order	U	Number of stream orders in each watershed	(Strahler 1952)
Stream number	N_u	Total stream number in each watershed	
Stream length (km)	L_u	Total stream length in each watershed	
Mainstream length (km)	L_{ms}	Mainstream length in each watershed	
Longest stream length (km)	L_{ls}	Longest stream length in each watershed	
Stream frequency	F_s	$F_s = N_u/A$	(Horton 1945)
1 st order stream frequency	F_1	$F_1 = 1^{\text{st}} \text{ order stream number} / A$	(Abdel-Fattah et al. 2017)
Drainage density	D_d	$D_d = L_u/A$	(Horton 1945)
Drainage texture	T	$T = D_d/F_s$	(Smith 1950)
Texture ratio	R_t	$R_t = N_u/P$	(Smith 1950)
Bifurcation ratio	R_b	$R_{bu} = N_u/N_{u+1}$	(Horton 1945)
Weighted mean bifurcation ratio	B_w	$B_w = \frac{1}{\sum_1^{\max(U)-1} (N_u + N_{u+1})} \sum_1^{\max(U)-1} R_{bu} (N_u + N_{u+1})$	(Shen et al. 2017)

208

209

210

211 **3.4. Mapping flash flood susceptible zones**

212 *3.4.1. Analysing relationships of morphometric parameters with flood susceptibility*

213 A rank (y) was assigned to each watershed according to the level of flood susceptibility using a relative
 214 ranking method in which 1 denotes a very low, and 5 a very high susceptibility in relation to the value
 215 of each morphometric parameter (x). Ranks were estimated by applying a linear interpolation technique
 216 proposed by Davis (2002). If the value of a morphometric parameter is positively correlated with the
 217 occurrence of a flash flood event, then equation 1 was used. Otherwise equation 2 was applied.

$$\text{If } y \propto x, \quad y'_n = \frac{(y_2 - y_1)(x'_n - x_{\min})}{(x_{\max} - x_{\min})} + y_1 \quad (1)$$

$$\text{If } y \propto \frac{1}{x}, \quad y'_n = \frac{(y_2 - y_1)(x'_n - x_{\max})}{(x_{\min} - x_{\max})} + y_1 \quad (2)$$

218 y'_n is the susceptibility rank of a parameter for the n^{th} watershed ($n = 1, 2, 3, \dots, 33$); the maximum
 219 rank $y_2 = 5$; minimum rank $y_1 = 1$; x'_n is the value of a parameter for the n^{th} watershed; x_{\max} is the
 220 maximum value of a parameter among all watersheds, and x_{\min} is the minimum value of a parameter
 221 among all watersheds.

222 As simulated hydrographs for the various watersheds within the region were not available, various
 223 studies depicting the pattern of relationships between flash floods and morphometric parameters were
 224 obtained and assessed. From these studies, the relationship of 22 (out of 29) morphometric parameters
 225 were determined (Table 3).

226 **Table 3 Relationship of various morphometric parameters with peak runoff**

Parameters	Relation with peak runoff	Reference
Basin area (A)	Positive correlation	(Abdel-Fattah et al. 2017; Youssef et al. 2011)
Basin length (L_b)	Positive correlation	(Abdel-Fattah et al. 2017; Bajabaa et al. 2014)
Time of concentration (T_c)	Negative correlation	(Youssef et al. 2011)
Mean elevation (H_m)	Positive correlation	(Abdel-Fattah et al. 2017; Bajabaa et al. 2014)
Total Basin Relief (R)	Positive correlation	(Abdel-Fattah et al. 2017; Bajabaa et al. 2014; Youssef et al. 2011)
Relief ratio (R_{hl})	Positive correlation	(Abdel-Fattah et al. 2017; Youssef et al. 2011)

Ruggedness number (R_n)	Positive correlation	(Farhan et al. 2017)
Mean basin slope (S_b)	Positive correlation	(Abdel-Fattah et al. 2017; Bajabaa et al. 2014; Schmidt et al. 2000)
Mainstream slope (S_{ms})	Positive correlation	(Abdel-Fattah et al. 2017)
Slope ratio (S_r)	Negative correlation	(Abdel-Fattah et al. 2017)
Longest stream slope (S_{ls})	Positive correlation	(Schmidt et al. 2000)
Form factor (F)	Positive correlation	(Abdelkareem 2017; Farhan et al. 2017; Youssef et al. 2011)
Compactness ratio (C)	Negative correlation	(Youssef et al. 2011)
Circularity ratio (R_c)	Positive correlation	(Abdel-Fattah et al. 2017; Farhan et al. 2017; Youssef et al. 2011)
Elongation ratio (R_e)	Negative correlation	(Bajabaa et al. 2014; Youssef et al. 2011)
Total stream number (N_u)	Positive correlation	(Abdel-Fattah et al. 2017; Youssef et al. 2011)
Total stream length (L_u)	Positive correlation	(Youssef et al. 2011)
Mainstream length (L_{ms})	Positive correlation	(Abdel-Fattah et al. 2017)
Stream frequency (F_s)	Positive correlation	(Youssef et al. 2011)
Drainage density (D_d)	Positive correlation	(Youssef et al. 2011)
Texture ratio (R_t)	Positive correlation	(Abdel-Fattah et al. 2017; Bajabaa et al. 2014)
Weighted mean bifurcation ratio (B_w)	Negative correlation	(Bajabaa et al. 2014)

227

228 3.4.2. Flood susceptibility mapping

229 Twenty-two flood susceptibility maps (constructed using the individual morphometric parameters)
 230 were used to estimate the total rank of each of the 33 watersheds. Here, the total rank of each watershed
 231 was estimated by adding all scores (rank) obtained for 22 morphometric parameters. The aggregated
 232 map was categorised (using the equation 1 formula) into five susceptibility classes - ‘very low’, ‘low’,
 233 ‘moderate’, ‘high’, and ‘very high’. In order to allow the resulting watershed-wise flood susceptibility
 234 maps to be easily interpreted by policy makers, the maps were disaggregated at the sub-district level,
 235 and the different sub-districts categorised according to the degree of flash flood potential. Since the
 236 river basins contained segments from 40 different sub-districts, the level of flood susceptibility at
 237 different sub-districts was noted as a percentage of the total area within the basin. The number of people

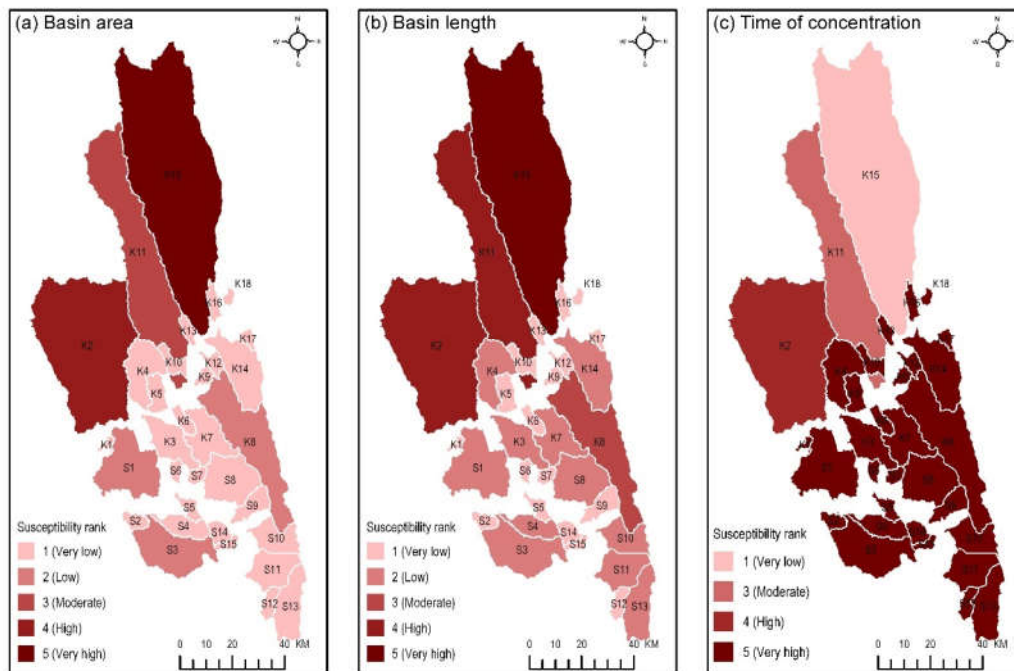
238 exposed to each category of flood susceptible zone was also calculated. This process was conducted for
 239 each sub-district. Gridded population data at 100 m resolution was obtained from Worldpop (WorldPop
 240 2017) in order to estimate flood-exposed population numbers

241 **4. Results and discussion**

242 **4.1. Relationships of morphometric parameters with flood susceptibility**

243 *4.1.1. Scale parameter*

244 The flash flood susceptibility ranking of different watersheds in relation to the three scale parameters
 245 noted previously is shown in Figure 3. The study delineated watersheds with areas ranging from 22 km²
 246 to 2,699 km², the range in size indicating the heterogeneous nature of the drainage basins. The larger
 247 area and greater length of the three watersheds in the Karnaphuli river basin (K2, K11, and K15) resulted
 248 in a flood susceptibility ranking of greater than 3. It should be noted, however, that a watershed with a
 249 larger area provides a greater degree of attenuation, reducing the susceptibility to flash flood events.
 250 For example, watershed K15 has the highest time of concentration i.e., 1562.69 min. Generally, the
 251 Karnaphuli river basin has relatively a greater time of concentration than the Sangu river basin (Table
 252 4).



253

254

Figure 3 Flash flood susceptibility ranking in relation to scale parameters

Table 4 Morphometric characteristics of the Karnaphuli and Sangu river basins in south-eastern Bangladesh

Watershed number	Morphometric parameters																					
	A	L _b	T _c	H _m	R	R _{hl}	R _n	S _b	S _{ms}	S _r	S _{ls}	F	C	R _c	R _e	N _u	L _u	L _{ms}	F _s	D _d	R _t	B _w
K1	21.6	7.5	47.98	6.3	21	2.79	0.06	1.75	0.63	0.36	1.94	0.49	3.41	0.09	0.70	71	59.2	5.9	3.28	2.74	1.26	4.96
K2	1733.1	90.7	435.21	41.4	254	2.80	0.70	4.90	1.67	0.341	1.67	0.27	2.24	0.20	0.52	5752	4786.2	47.3	3.32	2.76	17.41	5.58
K3	221.4	28.2	132.50	49.1	152	5.39	0.42	5.90	1.99	0.338	1.99	0.35	2.40	0.17	0.60	760	605.1	31.1	3.43	2.73	6.01	5.43
K4	260.0	30.9	81.50	61.1	249	8.06	0.67	8.29	2.00	0.241	2.00	0.35	2.41	0.17	0.59	842	701.4	24.5	3.24	2.70	6.11	5.35
K5	92.0	17.1	8.14	21.0	121	7.07	0.51	3.73	1.82	0.488	1.61	0.40	2.20	0.21	0.63	352	386.8	7.0	3.83	4.21	4.71	5.99
K6	54.2	12.7	0.69	72.3	244	19.26	0.63	10.58	3.19	0.301	7.04	0.43	2.13	0.22	0.66	189	140.2	3.6	3.49	2.59	3.40	4.65
K7	249.5	30.2	3.39	107.8	239	7.92	0.61	10.81	7.73	0.715	7.73	0.35	2.53	0.16	0.59	791	641.6	19.3	3.17	2.57	5.58	5.69
K8	723.9	55.2	25.67	174.4	224	4.06	0.52	8.57	7.23	0.844	7.23	0.30	2.60	0.15	0.55	2089	1685.3	49.8	2.89	2.33	8.42	5.23
K9	36.9	10.2	1.64	58.5	98	9.62	0.26	6.85	3.05	0.446	3.05	0.45	2.02	0.24	0.67	114	96.1	5.3	3.09	2.61	2.62	4.84
K10	67.2	14.3	9.20	83.0	224	15.64	1.20	8.63	1.51	0.175	5.31	0.42	2.32	0.19	0.65	245	358.6	6.2	3.65	5.34	3.63	7.73
K11	1310.7	77.4	672.23	87.2	224	2.89	0.64	7.64	0.74	0.096	2.39	0.28	3.18	0.10	0.53	4211	3717.8	25.9	3.21	2.84	10.30	5.53
K12	48.7	11.9	4.72	117.5	224	18.79	0.55	12.15	3.58	0.295	3.58	0.43	2.40	0.17	0.66	159	120.3	10.6	3.27	2.47	2.68	5.09
K13	44.5	11.3	1.20	116.6	224	19.78	0.55	10.52	4.14	0.393	8.76	0.44	2.12	0.22	0.66	130	109.1	6.2	2.92	2.46	2.60	6.55
K14	349.5	36.5	29.19	127.6	224	6.13	0.58	9.69	4.71	0.486	4.71	0.33	2.20	0.21	0.58	1069	908.8	34.5	3.06	2.60	7.32	5.50
K15	2698.5	116.6	1562.69	113.8	224	1.92	0.71	8.39	1.84	0.219	1.84	0.25	2.33	0.18	0.50	8966	8546.4	98.6	3.32	3.17	20.91	5.52
K16	53.9	12.6	2.60	134.8	224	17.74	0.57	12.45	5.10	0.41	5.10	0.43	2.19	0.21	0.66	162	136.1	11.2	3.01	2.53	2.84	6.37
K17	33.7	9.7	0.23	149.4	218	22.54	0.54	11.95	6.01	0.503	8.42	0.46	1.89	0.28	0.68	122	83.8	3.9	3.62	2.49	3.14	5.93
K18	23.3	7.8	0.19	64.8	162	20.65	0.47	7.83	1.51	0.192	4.35	0.48	2.11	0.23	0.69	79	68.1	0.9	3.39	2.92	2.19	5.00
S1	465.5	43.0	2.26	16.7	134	3.12	0.38	3.32	1.73	0.521	1.67	0.32	2.43	0.17	0.57	1645	1317.6	3.5	3.53	2.83	8.86	5.34
S2	52.6	12.5	1.06	24.2	86	6.90	0.23	4.43	1.83	0.413	2.20	0.43	2.31	0.19	0.66	168	142.7	2.6	3.20	2.71	2.83	5.68
S3	424.0	40.8	25.46	53.4	250	6.13	0.67	5.30	1.98	0.374	3.07	0.32	2.44	0.17	0.57	1371	1134.8	13.6	3.23	2.68	7.69	5.88
S4	134.0	21.2	43.29	66.5	249	11.75	0.65	6.55	1.94	0.296	3.44	0.38	2.56	0.15	0.62	428	352.1	17.4	3.19	2.63	4.08	5.87
S5	52.5	12.4	2.61	96.9	245	19.69	0.63	10.39	2.93	0.282	4.66	0.43	2.45	0.17	0.66	163	135.9	6.4	3.11	2.59	2.59	5.47
S6	34.7	9.8	0.71	51.1	106	10.78	0.29	8.96	4.41	0.492	4.41	0.46	1.94	0.27	0.68	113	94.5	5.0	3.26	2.72	2.79	5.52
S7	36.9	10.2	0.27	64.1	139	13.64	0.37	10.26	4.44	0.433	6.52	0.45	1.81	0.31	0.67	112	98.9	3.1	3.03	2.68	2.88	5.51
S8	326.4	35.1	1.28	140.1	242	6.89	0.62	9.67	7.81	0.808	10.74	0.34	1.87	0.29	0.58	1014	834.6	12.0	3.11	2.56	8.49	5.37
S9	107.7	18.7	1.13	204.9	246	13.14	0.55	6.99	12.31	1.761	12.31	0.39	2.06	0.23	0.63	286	238.9	17.8	2.66	2.22	3.77	5.55

S10	182.0	25.2	0.31	245.4	226	8.96	3.29	2.06	9.74	4.722	0.00	0.36	2.09	0.23	0.60	681	2649.9	7.4	3.74	14.56	6.80	38.53
S11	215.3	27.7	0.81	225.5	213	7.68	2.02	5.39	10.91	2.024	0.00	0.36	1.73	0.33	0.60	848	2038.2	13.3	3.94	9.47	9.43	11.64
S12	56.9	13.0	0.04	210.4	214	16.43	0.47	8.25	14.17	1.717	10.74	0.43	2.03	0.24	0.65	174	124.8	3.7	3.06	2.19	3.21	4.85
S13	244.8	29.8	0.47	234.8	193	6.47	1.64	4.38	15.44	3.528	0.00	0.35	1.89	0.28	0.59	834	2077.2	14.4	3.41	8.49	7.94	9.90
S14	59.6	13.4	0.02	162.6	218	16.30	0.52	12.20	9.67	0.792	11.81	0.42	1.84	0.30	0.65	183	143.4	1.7	3.07	2.41	3.64	5.48
S15	29.3	8.9	0.01	164.6	236	26.41	0.59	11.41	13.41	1.176	12.41	0.47	2.18	0.21	0.68	85	72.6	1.5	2.90	2.48	2.03	4.99

256

257 4.1.2. *Topographic characteristics*

258 A difference in elevation was also noted between the two river basins. The mean elevation of the
259 watersheds ranged in height from 6m to 255m. The eastern parts of the study area have a generally
260 higher elevation than those in the central and southwestern parts (Figure 1). Three watersheds (S10,
261 S11, S13) in the southern part of the study area received the highest flood susceptibility rank (Figure
262 4a). Basin relief, which represents the difference in elevation between the highest point and the basin
263 outlet, can determine the runoff potential of a watershed. A greater basin relief is less conducive to rapid
264 surface water infiltration, with the volume of the resulting overland flow/surface water (theoretically)
265 making an area more susceptible to flooding. A similar relationship exists between the relief ratio and
266 a flash flood event. While a higher susceptibility rank was estimated for most of the watersheds in terms
267 of basin relief, only a few of the smaller watersheds were deemed susceptible to flash flooding due to
268 their high relief ratio (Figure 4 (b-c)).

269 Of the watersheds examined, 29 have a ruggedness number of <1 . Two watersheds indicate a
270 ruggedness number from 1 to 2 and the remaining two watersheds have an extreme ruggedness number,
271 i.e. >2 (Table 4). The susceptibility rank of ≥ 3 was estimated for three watersheds (S10, S11, and S13)
272 (Figure 4d). Surfaces with a relatively high slope value characterize most of the region. The degree of
273 basin and mainstream slope, the longest stream, and basin size positively influences generation of
274 runoff. Figure 4 (e-h), shows flood-susceptible areas related to mean basin slope, mainstream slope, and
275 the longest stream slope. In relation to slope ratio, 23 watersheds received the highest flood
276 susceptibility rank due to a high slope ratio (Figure 4g).

277



278

279

Figure 4 Flash flood hazard ranking in relation to topographic parameters

280

4.1.3. Shape parameter

281

The estimated form factor values for all watersheds in the two basins were less than 0.79 (Table 4),

282

indicating that the shape of the individual basins is essentially circular. Based on this observation, 13

283

watersheds were given the highest susceptibility rank of 5 (Figure 5a). As the compactness ratio is

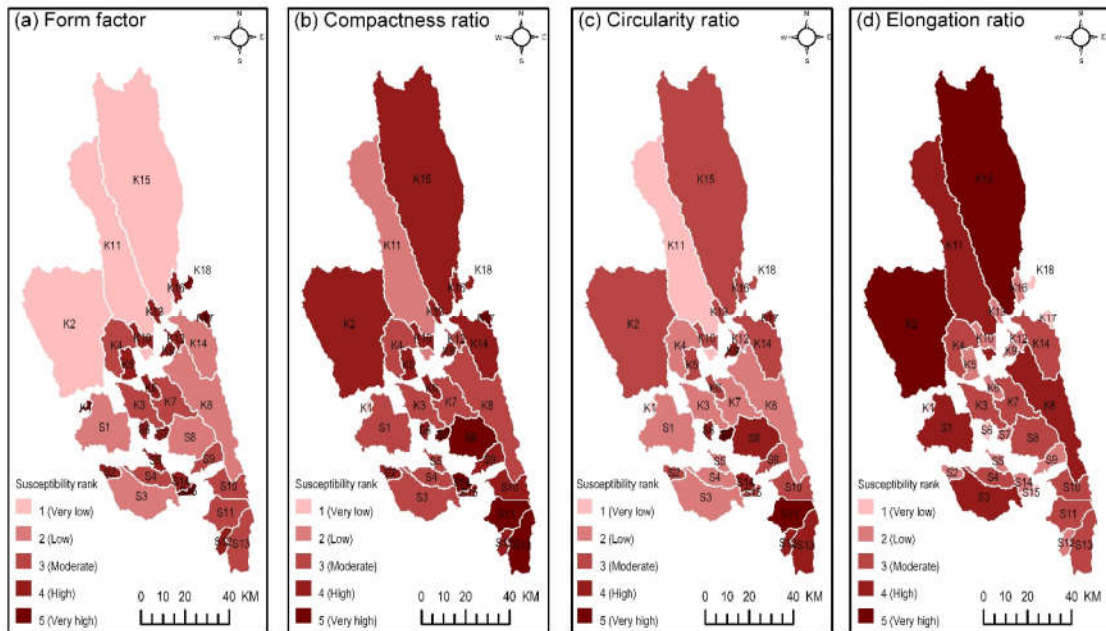
284

inversely related to flash flooding, the ratio was used to calculate a flash flood susceptibility rank of ≥ 3

285

for the 21 watersheds (Figure 5b). In relation to circularity ratio, 14 watersheds were found to be in

286 moderate to very high flood susceptible zones (Figure 5c). In regards the elongation ratio value, the
 287 flood potential in five watersheds is high (susceptibility rank ≥ 4) (Figure 5d).



288

289

Figure 5 Flash flood hazard ranking in relation to shape parameters

290

4.1.4. Characteristics of the stream systems

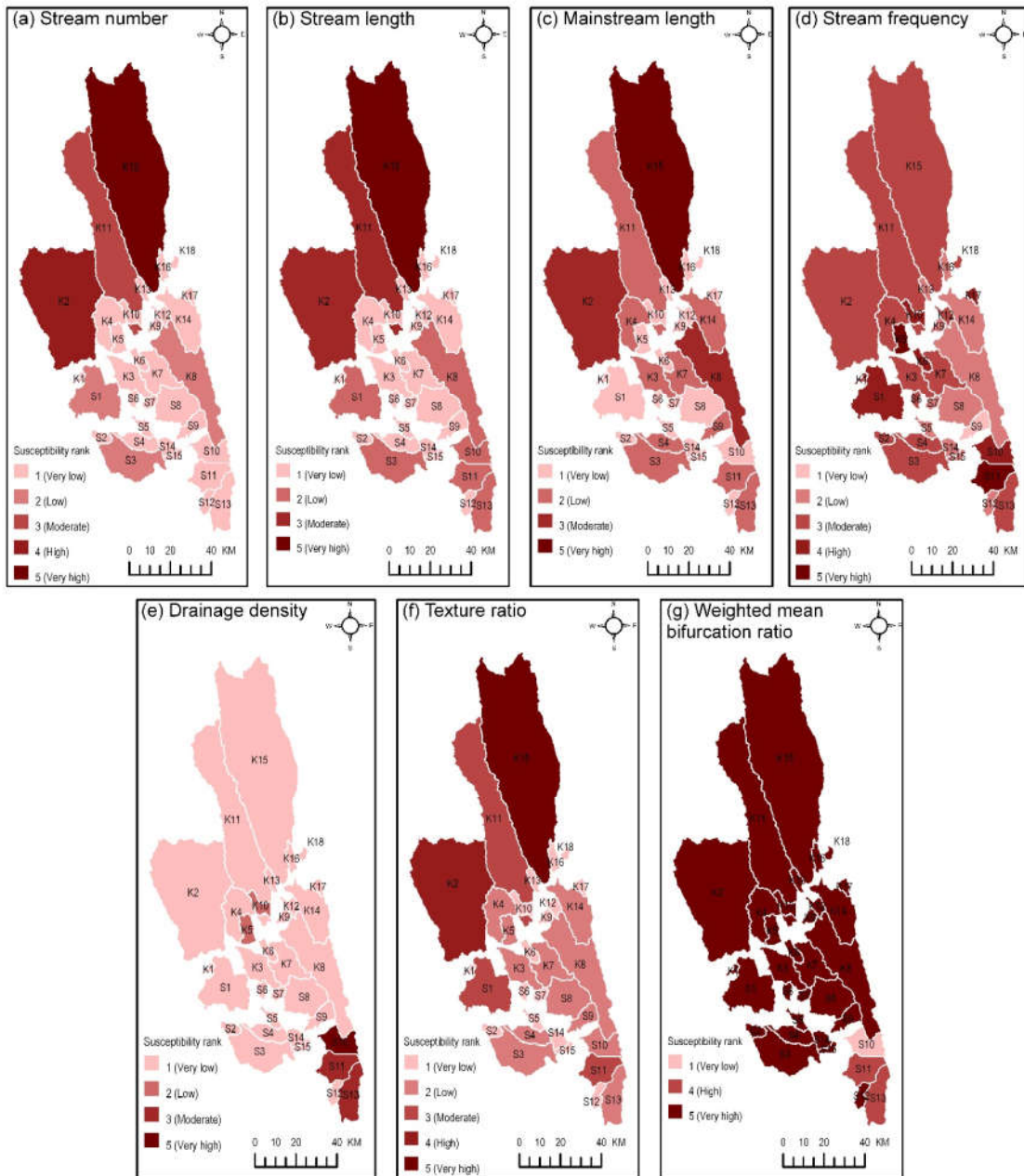
291

Depending on the size of a watershed, stream number in the two river basins ranged from 71 (K1) to
 292 8966 (K15). Likewise, total stream lengths and mainstream lengths vary from 59.2km to 8,546.4km
 293 and 0.88km to 98.57km, respectively (Table 4). In relation to stream number and total stream lengths,
 294 the three largest watersheds (K2, K11 and K15) indicate a high degree of flood susceptibility (Figure
 295 6(a-b)). Along with the watersheds K2 and K15, the higher mainstream length of K8 also makes it more
 296 susceptible to floods (Figure 6c).

297

Other characteristics of the stream systems used in the study include stream frequency, drainage density,
 298 texture ratio, and weighted mean bifurcation ratio. These parameters help explain the pattern of runoff
 299 generation that contributes to flash floods in the region as they are positively correlated with flash flood
 300 occurrence. In the watersheds of the two basins, the range of stream frequency and drainage density is
 301 found to be 2.66-3.94 and 2.19-14.56, respectively. With respect to stream frequency, 17 watersheds
 302 are susceptible to floods, as indicated by a rank of ≥ 3 (Figure 6d). Drainage density influences the
 303 occurrence of flash flood in three of the smaller watersheds (S10, S11, and S13) (Figure 6e). With
 304 regard to the texture ratio, four of the larger watersheds also appear prone to floods (Figure 6f). Most
 305 of the watersheds in the region have a weighted mean bifurcation ratio of 4-6, again indicating a high

306 degree of flood susceptibility. Watershed S10 received the lowest rank due to its high mean bifurcation
 307 ratio (Figure 6 g).



308

309

Figure 6 Flash flood hazard ranking in relation to the stream characteristics

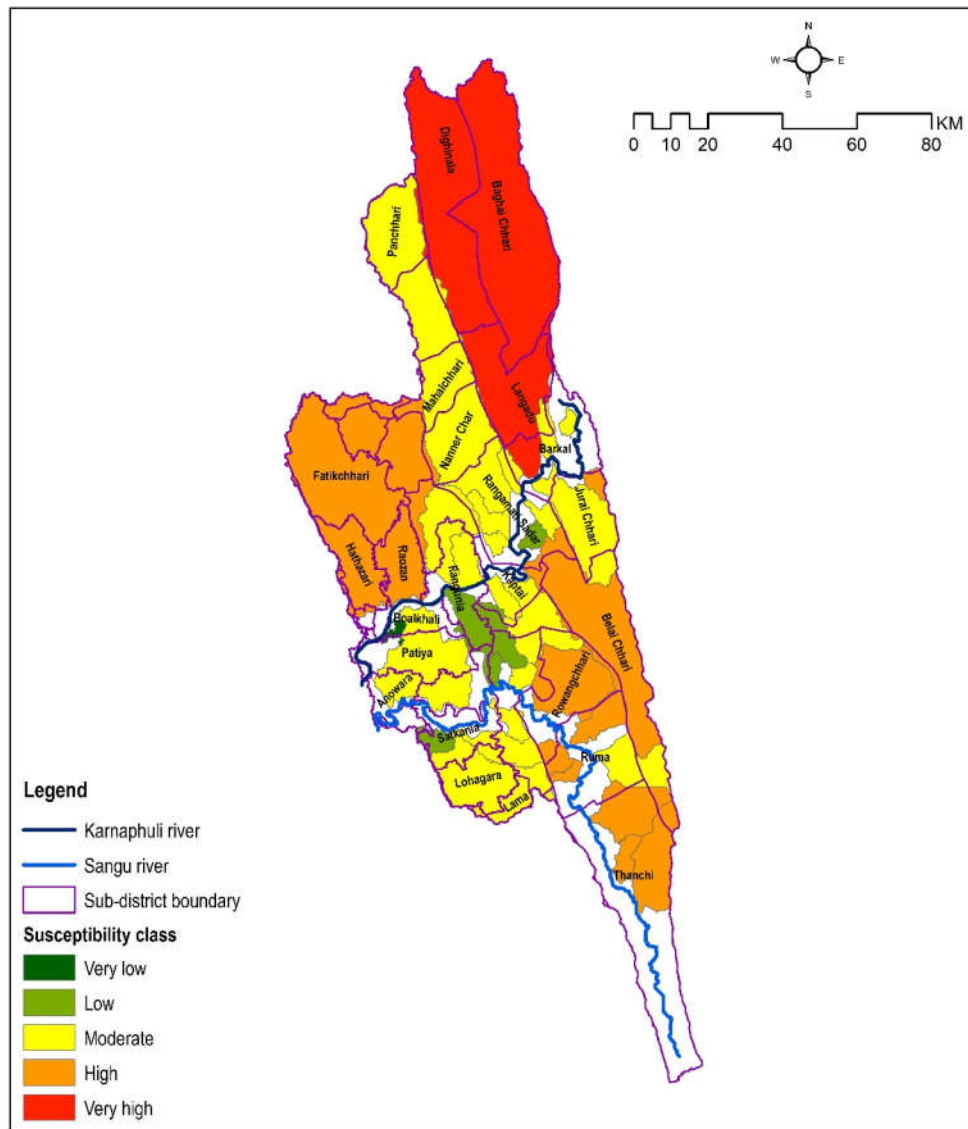
310

4.2. Flash flood susceptibility zones

311

A flash flood susceptibility map of the two river basins is shown in Figure 7. This indicates that several
 312 watersheds are highly susceptible to flash flood. For example, watershed K15 is located in a ‘very high’
 313 flood susceptibility category. A total of 10 watersheds have been categorised as ‘high’, while 17

314 watersheds are located in ‘moderate’ susceptibility zones. These results also indicate that only five
 315 watersheds have low flooding potential (as indicated by a susceptibility level of ‘low’ to ‘very low’) .
 316 The larger watersheds (those with a basin area greater than 100km² (Bajabaa et al. 2014)) also tend to
 317 receive a greater amount of precipitation. The larger watersheds also tend to have greater attenuation
 318 capacity, however the higher elevations associated with these areas, as well as greater slope angles and
 319 more varied relief, may lead to lower surface infiltration, greater overland flow and therefore an
 320 associated higher peak runoff. Due to these factors, most of the larger size watersheds were categorised
 321 as having ‘moderate’ to ‘very high’ susceptibility to flash floods.



322

323 Figure 7 Flash flood hazard map of the Karnaphuli and Sangu river basins

324 The watershed-based hazard assessment highlighted the flood susceptible zones. To enable the map to
 325 be used effectively for local hazard management, localities at the sub-district level were defined and

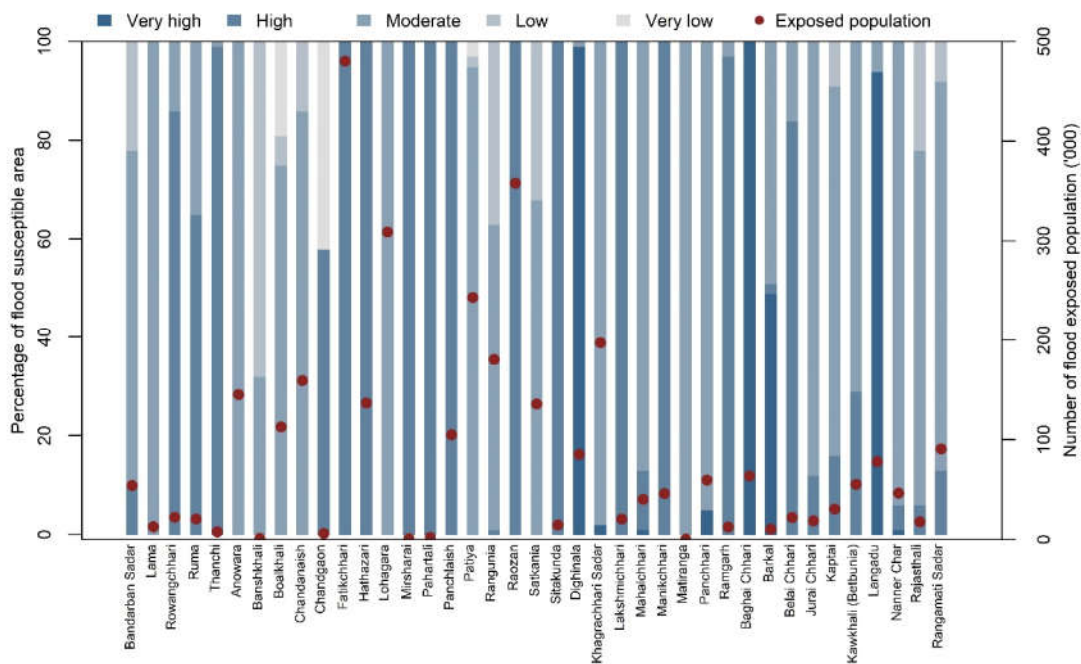
326 mapped and the number and location of people exposed to flash flood events was determined. The
 327 percentage of area within each identified flood-susceptible zone was calculated for each sub-district
 328 (Table 5). Most of these were categorized as ‘moderate’ or ‘high’ flood susceptible zones and had
 329 been affected by floods during different historical events. For instance, the whole area in Raozan sub-
 330 district is susceptible to a flood of ‘high’ severity. About 45,000 people in Raozan sub-district were
 331 affected during the 2015 event (ACAPS 2015). More than two-thirds of the area within 11 sub-districts
 332 of Chittagong district were identified as being susceptible to flash flood. This indicates a significant
 333 threat to the country’s trade and commerce, as this area is the commercial capital of Bangladesh. It
 334 should also be noted that, although the geomorphological characteristics of the area play a large part in
 335 the susceptibility to flash flooding events, anthropogenic activities such as hill cutting are also believed
 336 to have played a part in amplifying the recent impacts of floods (Sarker and Rashid 2013).

337 Table 5 Areas susceptible to flash floods in the two river basins

District	Sub-district	Percentage (%) of hazard area				
		Very low	Low	Moderate	High	Very high
Bandarban	Bandarban Sadar	0	22	68	10	0
	Lama	0	0	100	0	0
	Rowangchhari	0	0	14	86	0
	Ruma	0	0	35	65	0
	Thanchi	0	0	1	99	0
Chittagong	Anowara	0	0	100	0	0
	Banskhali	0	68	32	0	0
	Boalkhali	19	6	75	0	0
	Chandanaish	0	14	86	0	0
	Chandgaon	42	0	0	58	0
	Fatikchhari	0	0	0	100	0
	Hathazari	0	0	0	100	0
	Lohagara	0	0	100	0	0
	Mirsharai	0	0	0	100	0
	Pahartali	0	0	0	100	0
	Panchlaish	0	0	0	100	0
	Patiya	3	2	95	0	0
	Rangunia	0	37	62	1	0
	Raozan	0	0	0	100	0
	Satkania	0	32	68	0	0
Sitakunda	0	0	0	100	0	
Khagrachari	Dighinala	0	0	1	0	99
	Khagrachhari Sadar	0	0	98	0	2
	Lakshmichhari	0	0	0	100	0
	Mahalchhari	0	0	88	12	1
	Manikchhari	0	0	0	100	0
	Matiranga	0	0	100	0	0
Panchhari	0	0	95	0	5	

	Ramgarh	0	0	3	97	0
Rangamati	Baghai Chhari	0	0	0	0	100
	Barkal	0	0	49	1	49
	Belai Chhari	0	0	16	84	0
	Jurai Chhari	0	0	88	12	0
	Kaptai	0	9	75	16	0
	Kawkhali (Betbunia)	0	0	71	29	0
	Langadu	0	0	6	0	94
	Nanner Char	0	0	94	5	1
	Rajasthali	0	22	72	5	0
	Rangamati Sadar	0	8	79	12	0

338 The number of people exposed to different flash flood zones in the different sub-districts is shown in
 339 Figure 8. The term population exposure means the total number of people located within the ‘moderate’
 340 to ‘very high’ level susceptibility zones. The analysis showed that about 0.48 million people in
 341 Fatikhchhari sub-district live in the “very high” flood susceptible zone. The 2015 event affected
 342 approximately 17,000 people in this sub-district and damaged 200 houses (ACAPS 2015). Likewise,
 343 about 0.36 million people in Raozan sub-district live in ‘high’ level flood susceptible areas. Despite the
 344 flood susceptibility level of the K15 watershed being very high, the number of people actually exposed
 345 to flooding is low since relatively few people live in this area. Other sub-districts located in K15 (with
 346 associated figures for population exposure) are Dighinala (85,000), Baghai Chhari (64,000) and
 347 Langadu (78,000).



348

349

Figure 8 Number of people exposed to flash flood in different sub-districts

350 **5. Conclusion**

351 This GIS-based study defined morphometric parameters accountable for flash flood hazard in
352 watersheds of the Karnaphuli and Sangu river basins. A digital elevation model was obtained and used
353 to derive drainage networks and river basins. The study estimated 22 morphometric parameters and
354 grouped them into four categories in order to examine the parameter relationships with peak runoff
355 flows which contribute to flash flooding. These were then used to create a map of flash flood
356 susceptibility based on the sub-district boundaries. Overlying the sub-district map on gridded
357 population data assisted in identifying the population exposure numbers within the various zones.

358 The study results indicated that flash flood hazards are mainly associated with the volume of water
359 runoff, the associated water velocity and the amount of infiltration occurring during the surface water
360 flow. The large watersheds receive a higher amount of precipitation, resulting in a greater volume of
361 runoff. Elevation, slope angle and basin relief characteristics also influence the flood susceptibility of
362 these basins. The study also indicated that hilly areas within the study region are at risk of severe
363 inundation and so it is fortunate that relatively few people live in these areas. A substantial number of
364 people, however, do live in the ‘high’ flood susceptible zones in the various sub-districts and are
365 therefore exposed to the associated increased risks to lives, livelihood and property by flood events.

366 Flash flood susceptibility mapping, through the use of morphometric analysis, overcomes the limitation
367 of hydrological flood models which are time-consuming to construct, and which are difficult to apply
368 over larger areas (Youssef et al. 2011). This study does, however, have some limitations. Relative flood
369 risk and the ranking of flood susceptibility in various watersheds were determined, with a focus on
370 assessing flood susceptibility at the watershed scale. The inability to obtain actual flood data, however,
371 makes it difficult to map flood susceptibility at a microscale. Although remote sensing data (such as
372 Landsat images) provides information which can be useful for observing flood inundation (Rahman and
373 Di 2017), the presence of cloud cover during the monsoon season (Adnan et al. 2019) makes it very
374 difficult to accurately observe flash flood events with satellite data. An additional factor is the speed of
375 rise and subsidence of water during a flash flood event, as opposed to the longer time taken by riverwater
376 flooding events.

377 Despite the limitations noted above, the study does provide an overview of the flash flood hazard zones
378 identified in a region of national importance, and the associated level of exposure of the population to
379 these hazards. A focus on flash flood susceptibility mapping at the sub-district level also enables the
380 deployment of flood risk mitigation strategies by the local organizations responsible for watershed
381 management. A knowledge of the flood susceptibility level of each watershed/sub-district can be of
382 great benefit in the development of any such strategies. The study also provides some direction for
383 future research. Synthetic-aperture radar (SAR) images, which have the ability to penetrate cloud, can
384 be employed to observe flash floods and map microscale flood susceptibility (Rahman and Di 2017).

385 Hydrologically dynamic modelling could also be used in the highly flood-susceptible zones to simulate
386 potential inundation areas.

387 **Acknowledgement**

388 We thank the anonymous reviewers for their careful reading of our manuscript and insightful comments
389 and suggestions.

390 **6. References**

- 391 Abdel-Fattah M, Saber M, Kantoush SA, Khalil MF, Sumi T, Sefelnasr AM (2017) A hydrological
392 and geomorphometric approach to understanding the generation of wadi flash floods Water
393 (Switzerland) 9 doi:10.3390/w9070553
- 394 Abdelkareem M (2017) Targeting flash flood potential areas using remotely sensed data and GIS
395 techniques Natural Hazards 85:19-37 doi:10.1007/s11069-016-2556-x
- 396 Abdullah AYM, Masrur A, Adnan MSG, Baky MAA, Hassan QK, Dewan A (2019) Spatio-Temporal
397 Patterns of Land Use/Land Cover Change in the Heterogeneous Coastal Region of
398 Bangladesh between 1990 and 2017 Remote Sensing 11:790
- 399 ACAPS (2015) Flash Floods in Cox's Bazar, Bandarban and Chittagong Districts June-July 2015.
400 Assessment Capacities Project
- 401 Adnan MSG, Haque A, Hall JW (2019) Have coastal embankments reduced flooding in Bangladesh?
402 Science of the Total Environment 682:405-416 doi:10.1016/j.scitotenv.2019.05.048
- 403 Adnan SG, Kreibich H (2016) An evaluation of disaster risk reduction (DRR) approaches for coastal
404 delta cities: a comparative analysis Natural Hazards 83:1257-1278
- 405 Ahmed B, Dewan A (2017) Application of bivariate and multivariate statistical techniques in
406 landslide susceptibility modeling in Chittagong City Corporation, Bangladesh Remote
407 Sensing 9 doi:10.3390/rs9040304
- 408 Bajabaa S, Masoud M, Al-Amri N (2014) Flash flood hazard mapping based on quantitative
409 hydrology, geomorphology and GIS techniques (case study of Wadi Al Lith, Saudi Arabia)
410 Arabian Journal of Geosciences 7:2469-2481 doi:10.1007/s12517-013-0941-2
- 411 BBS (2015) Bangladesh Disaster-related Statistics 2015. Climate Change and Natural Disaster
412 Perspectives Bangladesh Bureau of Statistics (BBS), Ministry of Planning, Dhaka,
413 Bangladesh
- 414 Bhatt S, Ahmed SA (2014) Morphometric analysis to determine floods in the Upper Krishna basin
415 using Cartosat DEM Geocarto International 29:878-894 doi:10.1080/10106049.2013.868042
- 416 Biswas S, Vacik H, Swanson ME, Haque SS (2012) Evaluating integrated watershed management
417 using multiple criteria analysis—a case study at Chittagong Hill Tracts in Bangladesh
418 Environmental monitoring and assessment 184:2741-2761
- 419 Brammer H (1990) Floods in Bangladesh: I. Geographical background to the 1987 and 1988 floods
420 Geographical Journal 156:12-22 doi:10.2307/635431
- 421 Bronstert A, Niehoff D, Bürger G (2002) Effects of climate and land-use change on storm runoff
422 generation: present knowledge and modelling capabilities Hydrological processes 16:509-529
- 423 Choudhury NY, Paul A, Paul BK (2004) Impact of costal embankment on the flash flood in
424 Bangladesh: A case study Applied Geography 24:241-258 doi:10.1016/j.apgeog.2004.04.001
- 425 Collier C (2007) Flash flood forecasting: What are the limits of predictability? Quarterly Journal of
426 the royal meteorological society 133:3-23
- 427 Davis J (2002) Statistics and Data Analysis in Geology - 3rd Edition. John Wiley and Sons, USA
- 428 Dewan A (2013) Floods in a megacity: geospatial techniques in assessing hazards, risk and
429 vulnerability (pp. 119-156). Dordrecht: Springer.
- 430 Dewan TH (2015) Societal impacts and vulnerability to floods in Bangladesh and Nepal Weather and
431 Climate Extremes 7:36-42 doi:https://doi.org/10.1016/j.wace.2014.11.001

432 Diakakis M (2011) A method for flood hazard mapping based on basin morphometry: application in
433 two catchments in Greece *Natural Hazards* 56:803-814 doi:10.1007/s11069-010-9592-8

434 Elnazer AA, Salman SA, Asmoay AS (2017) Flash flood hazard affected Ras Gharib city, Red Sea,
435 Egypt: a proposed flash flood channel *Natural Hazards* 89:1389-1400 doi:10.1007/s11069-
436 017-3030-0

437 Farhan Y, Anaba O, Salim A (2017) Morphometric Analysis and flash floods assessment for drainage
438 basins of the Ras En Naqb Area, South Jordan using GIS Applied Morphometry and
439 Watershed Management Using RS, GIS and Multivariate Statistics (Case Studies):413

440 Field CB, Barros V, Stocker TF, Dahe Q (2012) Managing the risks of extreme events and disasters to
441 advance climate change adaptation: special report of the intergovernmental panel on climate
442 change. Cambridge University Press,

443 Global Active Archive of Large Flood Events (2018) Dartmouth Flood Observatory, University of
444 Colorado. <http://floodobservatory.colorado.edu/Archives/index.html>.

445 Horton RE (1932) Drainage-basin characteristics *Eos, Transactions American Geophysical Union*
446 13:350-361 doi:10.1029/TR013i001p00350

447 Horton RE (1945) Erosional development of streams and their drainage basins; Hydrophysical
448 approach to quantitative morphology *Bulletin of the Geological Society of America* 56:275-
449 370 doi:10.1130/0016-7606(1945)56[275:EDOSAT]2.0.CO;2

450 Hughes RM, Kaufmann PR, Weber MH (2011) National and regional comparisons between Strahler
451 order and stream size *Journal of the North American Benthological Society* 30:103-121
452 doi:10.1899/09-174.1

453 Kabenge M, Elaru J, Wang H, Li F (2017) Characterizing flood hazard risk in data-scarce areas, using
454 a remote sensing and GIS-based flood hazard index *Natural Hazards* 89:1369-1387

455 Kamal ASMM, Shamsudduha M, Ahmed B, Hassan SMK, Islam MS, Kelman I, Fordham M (2018)
456 Resilience to flash floods in wetland communities of northeastern Bangladesh *International*
457 *Journal of Disaster Risk Reduction* 31:478-488 doi:10.1016/j.ijdrr.2018.06.011

458 Kron W (2005) Flood risk= hazard• values• vulnerability *Water International* 30:58-68

459 Land resource information management system (2014) Bangladesh Agricultural Research Council
460 (BARC). <http://www.barc.gov.bd>.

461 Lin L et al. (2019) Improvement and Validation of NASA/MODIS NRT Global Flood Mapping
462 *Remote Sensing* 11:205

463 Melton MA (1957) An analysis of the relations among elements of climate, surface properties, and
464 geomorphology. COLUMBIA UNIV NEW YORK,

465 Planchon O, Darboux F (2002) A fast, simple and versatile algorithm to fill the depressions of digital
466 elevation models *Catena* 46:159-176

467 Plate EJ (2002) Flood risk and flood management *Journal of Hydrology* 267:2-11

468 Rahman M, Di L, Yu E, Lin L, Zhang C, Tang J (2019) Rapid flood progress monitoring in cropland
469 with NASA SMAP Remote Sensing 11:191

470 Rahman MS, Ahmed B, Di L (2017) Landslide initiation and runoff susceptibility modeling in the
471 context of hill cutting and rapid urbanization: a combined approach of weights of evidence
472 and spatial multi-criteria *Journal of Mountain Science* 14:1919-1937

473 Rahman MS, Di L (2017) The state of the art of spaceborne remote sensing in flood management
474 *Natural Hazards* 85:1223-1248

475 Rahman R, Salehin M (2013) Flood Risks and Reduction Approaches in Bangladesh. In: Shaw R,
476 Mallick F, Islam A (eds) *Disaster Risk Reduction Approaches in Bangladesh*. Springer,
477 Tokyo, pp 65-90

478 Rai PK, Mohan K, Mishra S, Ahmad A, Mishra VN (2017) A GIS-based approach in drainage
479 morphometric analysis of Kanhar River Basin, India *Applied Water Science* 7:217-232
480 doi:10.1007/s13201-014-0238-y

481 Sarker AA, Rashid AKMM (2013) Landslide and Flashflood in Bangladesh. In: Shaw R, Mallick F,
482 Islam A (eds) *Disaster Risk Reduction Approaches in Bangladesh*. Springer Japan, Tokyo, pp
483 165-189. doi:10.1007/978-4-431-54252-0_8

484 Schmidt J, Hennrich K, Dikau R (2000) Scales and similarities in runoff processes with respect to
485 geomorphometry *Hydrological Processes* 14:1963-1979 doi:doi:10.1002/1099-
486 1085(20000815/30)14:11/12<1963::AID-HYP48>3.0.CO;2-M

487 Schumm SA (1956) Evolution of drainage systems and slopes in badlands at Perth Amboy, New
488 Jersey *Bulletin of the Geological Society of America* 67:597-646 doi:10.1130/0016-
489 7606(1956)67[597:EODSAS]2.0.CO;2

490 Seibert J, McGlynn BL (2007) A new triangular multiple flow direction algorithm for computing
491 upslope areas from gridded digital elevation models *Water Resources Research* 43
492 doi:10.1029/2006WR005128

493 Shen X, Anagnostou EN, Mei Y, Hong Y (2017) A global distributed basin morphometric dataset
494 *Scientific Data* 4:160124 doi:10.1038/sdata.2016.124

495 Smith KG (1950) Standards for grading texture of erosional topography *American Journal of Science*
496 248:655-668

497 Strahler AN (1952) Hypsometric (area-altitude) analysis of erosional topography *Bulletin of the*
498 *Geological Society of America* 63:1117-1142 doi:10.1130/0016-
499 7606(1952)63[1117:HAAOET]2.0.CO;2

500 Strahler AN (1957) Quantitative analysis of watershed geomorphology *Eos, Transactions American*
501 *Geophysical Union* 38:913-920 doi:doi:10.1029/TR038i006p00913

502 Stralher A (1964) Quantitative geomorphology of drainage basins and channel net work *Handbook of*
503 *Applied Hidrology*:4-76

504 Wiczorek ME (2012) Flow-Based Method for Stream Generation in a GIS *United States Geological*
505 *Survey August* 6

506 WorldPop (2017) Bangladesh 100m Population, Version 2 University of Southampton DOI:
507 105258/SOTON/WP00533

508 Youssef AM, Pradhan B, Hassan AM (2011) Flash flood risk estimation along the St. Katherine road,
509 southern Sinai, Egypt using GIS based morphometry and satellite imagery *Environmental*
510 *Earth Sciences* 62:611-623 doi:10.1007/s12665-010-0551-1